Tunnel Display for Four-Dimensional Fixed-Wing Aircraft Approaches

Arthur J. Grunwald*
Technion—Israel Institute of Technology, Haifa, Israel

A computer-generated perspective tunnel display for the four-dimensional fixed-wing aircraft approach to landing is evaluated. Attention is focused on the development and experimental evaluation of superimposed predictor symbology. It is investigated whether more complex predictive information, such as a perspective vehicle symbol predicting the future position as well as future attitude angles of the vehicle contributes to a better system response, as compared to a flat predictor cross, indicating the predicted vehicle position only. Methods for utilizing the predictor symbol motions in controlling the forward velocity of the aircraft in four-dimensional approaches are investigated. Simulator tests show that the complex perspective vehicle symbol yields a decrease in bank-angle activity as compared to a flat predictor cross, but yields, in most cases, generally larger lateral and vertical deviations. It is also shown that the perspective vehicle symbol motions can be utilized successfully in controlling the forward velocity of the aircraft, yielding a sufficiently accurate velocity control response, without affecting path following performance. Since the flat predictor cross already yields a satisfactory response, the advantage of the perspective vehicle symbol over the flat predictor cross is marginal, so that for graphic systems with limited computation power the flat predictor cross is recommended. Although the tunnel display is shown to yield a very satisfactory response and pilot acceptance in the lateral axis of control, the vertical axis of control is found to lack sensitivity to variations in the vertical path angle, and the development of superimposed symbology, enabling a more accurate vertical path-angle control, is recommended.

Introduction

THE advent of fast, low-cost microprocessors and new developments in cathode-ray tube (CRT) and graphics display technology have largely encouraged the development of computer-generated flight displays. The excessive workload present in the conventional instrument approach to landing has led to the development of pictorial flight-path displays. These displays present an image analogous to the "through-the-windshield" visual field, and show the horizontal and vertical situation of the aircraft with respect to a pictorially presented commanded flight path. Thus both lateral and vertical position information, as well as lateral and vertical commanded path information, are integrated in one display format.

Various formats of pictorial displays have been developed and experimentally evaluated. Sidorsky and Allen[1] have evaluated advanced displays for submarine integrated control. LaRussa,[2] Van Houtte,[3] and Eisele et al.,[4] have evaluated pictorial displays for a straight approach to landing of fixed-wing aircraft, whereas Murphy and Greif[5] have evaluated these displays for VTOL aircraft. Pictorial displays for a curved flight-path have been developed by Wilckens and Schattenmann,[6,7] in which the commanded path is represented by a channel as viewed from the actual aircraft position, and by Knox and Leavitt,[8] in which the commanded path is a "pathway-in-the-sky" as viewed "outside-in" from above and behind the actual aircraft position. Kraiss and Schubert[9] use the image of a channel, and Adams and Lallman[10] use that of a box for displaying commanded path information. However, in contrast to the previous displays in which the tunnel or channel is fixed in the Earth-reference system, these images move along with the vehicle at a fixed distance ahead. Predictor displays have been developed and evaluated by Kelley[11] and Smith and Kennedy.[12,13]

This paper extends the work done in the references mentioned above and deals specifically with the development and experimental evaluation of predictive information superimposed on the display. The tunnel display, developed in a previous work[14] for the steep and strongly curved three-dimensional helicopter approach to landing, is implemented in this paper for a four-dimensional fixed-wing commercial aircraft approach to landing. It is shown[14] that a predictor cross, superimposed on the tunnel image, predicting the vehicle position a given time in advance, both furnishes the system with the necessary damping cues and assists the pilot in coping with the trajectory curvature forcing function by providing the correct control command information. In this paper the involvement of the predictive information is extended further. Instead of the previously used flat predictor cross,[14] a perspective vehicle symbol is presented, displaying not only the future vehicle position, but also the future vehicle attitude angles. In addition to providing damping cues and command information, the predictive information also is utilized in controlling the forward velocity of the aircraft in four-dimensional approaches. This is accomplished by using the changes in predictor distance, resulting from changes in forward velocity, as a control cue. The main motivation for using the predictive information for controlling the forward velocity is that all control information necessary for lateral, vertical, and velocity control remains concentrated in the central area of the display.

Description of the Display

The various configurations of the tunnel display that were investigated are summarized below.

Tunnel with Perspective Vehicle Symbol and Forward Velocity Reference

The basic tunnel display configuration for the four-dimensional approach to landing is shown in Fig. 1. The winding and descending three-dimensional approach path is presented to the pilot as a "tunnel-in-the-sky," which is inertially fixed in space. In order to follow the desired approach path, the pilot must keep the vehicle inside the tunnel.

Submitted Nov. 30, 1982; revision received June 7, 1983.

*Senior Lecturer, Control Systems Engineering, Department of Aeronautical Engineering.

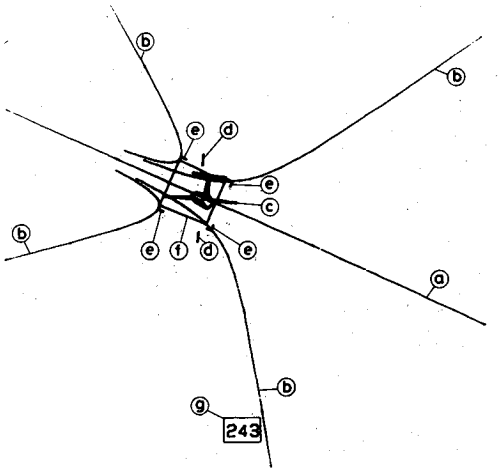

Fig. 1 Tunnel display with perspective vehicle symbol, $D_0 = 1500$ ft.

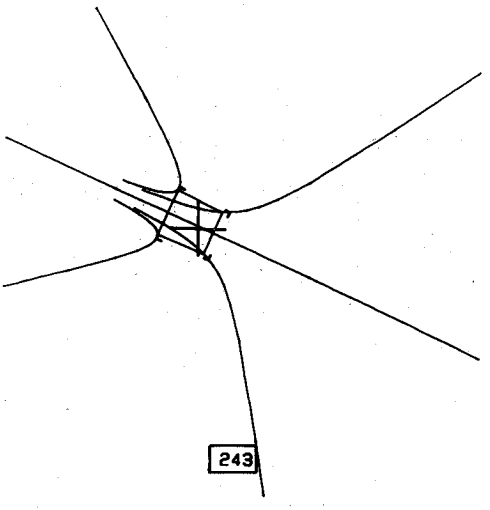

Fig. 2 Tunnel display with flat predictor cross, $D_0 = 1500$ ft.

The image shown in Fig. 1 is analogous to the "through-the-windshield" visual field with a ±45 deg field-of-view and shows the horizon [indicated by (a) in Fig. 1] and the tunnel image with cornerlines [indicated by (b) in Fig. 1.] The tunnel has a constant and square cross section 300 ft wide which remains upright at all times with respect to inertial space and thus parallel to the horizon, referred to hereafter as "upright tunnel". The tunnel width of 300 ft is expected to provide sufficient separation from other vehicles in complicated future air traffic control patterns. Analogous to the natural visual field, a left bank is visualized by a clockwise rotation of the image about the monitor center and a nose-up pitch motion is visualized by a vertical downward displacement of the image, perpendicular to the horizon. The cornerlines of the tunnel are composed of straight-line segments 200 ft long. The points at which these lines interconnect appear as bright spots. While moving through the tunnel these spots contribute highly to the impression of forward motion.

Superimposed on the tunnel image is the perspective vehicle symbol [indicated by (c) in Fig. 1]. The center of gravity of the vehicle symbol indicates the predicted vehicle location T s in advance, and the angular orientation of the symbol indicates the predicted attitude angles of the vehicle. The predictor motion laws, as well as a graphical description of the predictor, are given in the Appendix. The predictor symbol is located at a distance D ahead of the vehicle, where D is predicted from the actual vehicle velocity, vehicle states, and control inputs T s in the future. For the given vehicle dynamics, airspeed, and control task, T is chosen in the range between 4 and 7 s. The wing span of the vehicle symbol is identical to the tunnel width, i.e. 300 ft, which is about three times that of the wing span of the actual aircraft. The bars [indicated by (d) in Fig. 1] are positioned on the vertical axis of the vehicle symbol and serve as a vertical reference. The space between these bars is identical to the height of the square, i.e., 300 ft. In contrast to the tunnel image, the vehicle symbol is not a "wire-frame" structure since the hidden lines are removed. A wire-frame symbol is ambiguous and can be interpreted equally well pointing towards the observer as well as away from the observer, a fact which may lead to confusion and even to control reversals.

The four corner "tick-marks" [indicated by (e) in Fig. 1] indicate a cross section of the tunnel, which moves along, ahead of the vehicle, at the same distance D as the predictor symbol. The solid square [indicated by (f) in Fig. 1] is a cross section of the tunnel as well, but is positioned at reference predictor distance $D_0 = T/V_0$ ahead, where V_0 is the desired velocity. Since the solid square corresponds to the desired velocity and the corner tick-marks to the actual velocity, the velocity of the vehicle in four-dimensional approaches is controlled by matching the tick-marks to the solid square. In addition, an increase in velocity and, thus, an increase in predictor distance, manifests as an apparent shrinking in size of the predictor symbol and a decrease in velocity manifests as an apparent growing in size of the predictor symbol. In order to distinguish more clearly between the tick-marks and the solid square, the tick-marks are drawn at three times the intensity of the solid square. Furthermore, the tick-marks are blinked at a 3 Hz frequency when the forward velocity error exceeds a 5 ft/s threshold.

The forward velocity of the vehicle is displayed digitally as well by the digital readout box in the bottom-center of the display.

Tunnel with Flat Predictor Cross

The tunnel display with a flat predictor cross is shown in Fig. 2. The height and width of the cross are identical to the tunnel square, i.e., 300 ft. The center of the cross coincides with the center of gravity of the perspective vehicle symbol. However, in contrast to the perspective symbol, the predictor cross remains upright at all times with respect to the display reference frame and thus does not display the future attitude angles of the vehicle.

Roll-Stabilized Tunnel

The toll-stabilized tunnel display is shown in Fig. 3. In contrast to the "inside-out" roll version of the display, the horizon and tunnel image remain level at all times on the display and only the vehicle symbol is rolling. However, a disadvantage of this configuration is that without further augmentation, the actual bank-angle is no longer available since the vehicle symbol displays the predicted bank-angle rather than the actual bank-angle. The bank-angle information is correct in the steady state only, since only then the predicted and actual bank-angle are identical.

"Banked" Tunnel

A configuration of the roll-stabilized tunnel display, which provides a bank-angle command by banking the tunnel elements in curves, is shown in Fig. 4, and is referred to hereafter as "banked tunnel." The trajectory bank-angle corresponds to the bank-angle which is required in a coordinated turn at the desired vehicle velocity. In level flight, as well as in a steady turn flown at the correct speed, the actual bank-angle will be identical to the commanded trajectory bank-angle, and thus the wings of the perspective vehicle symbol will be parallel to the base of the tunnel square.

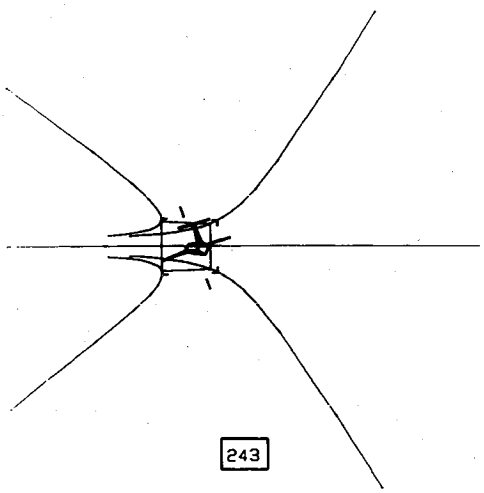

Fig. 3 Roll-stabilized tunnel display, $D_0 = 1500$ ft.

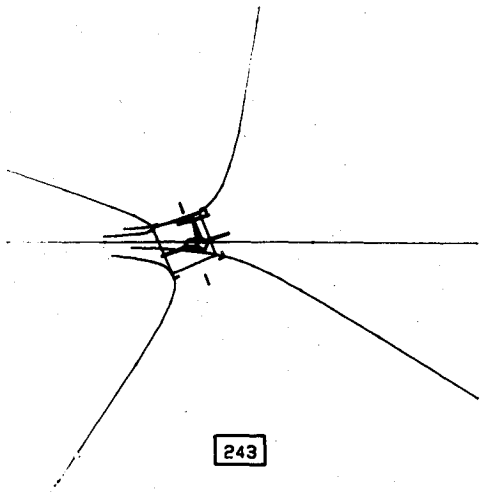

Fig. 4 Banked tunnel, roll-stabilized version.

The roll-version of the banked tunnel is shown in Fig. 5. In a steady turn both the wings of the vehicle symbol as well as the square will be parallel to the base of the monitor. In this situation, the inclined horizon provides the only actual bank-angle information.

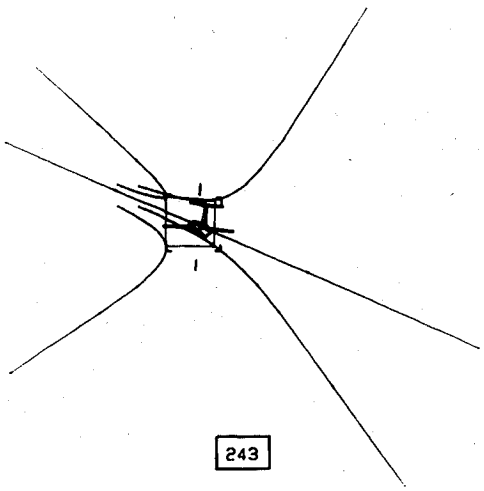

Fig. 5 Banked tunnel, roll version.

Experimental Evaluation

Experimental Program

In the experimental program two fixed-base simulator facilities were used: 1) a low-cost visual simulation system, and 2) an authentic full-scale Boeing 737 simulator cockpit. With the low-cost visual simulation system an extensive quantitative evaluation took place with nonpilot subjects, whereas with the full-scale cockpit a limited number of preliminary qualitative simulator tests were carried out by experienced research pilots.

The objectives of the experimental program were:

1) To compare the performance of the tunnel display with perspective vehicle symbol with the one with flat predictor cross.

2) To evaluate the use of the perspective vehicle symbol with velocity tick-marks for controlling the forward velocity of the aircraft.

3) To investigate the effect of the tunnel width.

4) To evaluate the effect of displaying the commanded bank-angle by banking the tunnel elements in curves, both for the roll version and the roll-stabilized version of the display.

Experimental System

The low-cost visual simulation system included two EAI-580 hybrid-analog computers slaved to a Data General Corporation Eclipse computer with 128-K extended memory for computing the vehicle response and generating the dynamic images of the various display configurations. Optimized, efficient assembly-language-written graphics software was developed for generating the dynamic images with suffficient update rate. The generated images, digitally coded in a sequence of move/draw commands, were translated into analog voltages by a Hewlett-Packard HP-1350A graphics translator and presented to the pilot on a HP-1310A monitor, measuring 19 in. diagonally, as a stroke-written single-color image.

Pilot commands were generated by a two-axis spring-loaded control stick and an unloaded throttle control lever. The range of the control stick was +2 to −2 cm and the maximum spring torque was 0.3 Nm for both axes. A forward stick displacement created a pitch motion and a lateral stick displacement created a roll motion. Rudder pedals were not present and turn coordination was carried out by a stability augmentation system. The range of the throttle control lever was +8 to −8 cm.

The full-scale B-737 cockpit was connected both to a CDC Cyber 175 computer for computing the vehicle motions of a B-737 aircraft in real-time, and to an Adage Graphics Terminal AGT 130 for generating the displays. The images were displayed in the cockpit on an 8-in. monitor. Except for the addition of pitch and roll scales, the display formats were identical to the ones used with the low-cost simulation system.

Description of the Experiments

The experiments were concerned with the approach to landing in the range 30,000-1,000 ft from the touchdown point. With the low-cost simulation system the vehicle dynamics of a DC-8 were simulated. Lateral and longitudinal dynamics were fully decoupled and linearized about a nominally straight and level flight trim condition at a nominal airspeed of 243.5 ft/s with the flaps extended to 35 deg. The stability derivatives are derived from Ref. 15. The vehicle was equipped with a stability augmentation system including loop closures of roll rate on aileron, yaw rate and sideslip angle on rudder, and pitch rate and angle of attack on elevator. The complete vehicle model with stability augmentation system is described in Ref. 16. A planview of the desired trajectory is shown in Fig. 6 and the vertical descent profile along the trajectory is shown in Fig. 7. The commanded velocity V_o was set at 243.5 ft/s over the complete approach path. A description of the two types of experiments that were conducted is given hereafter.

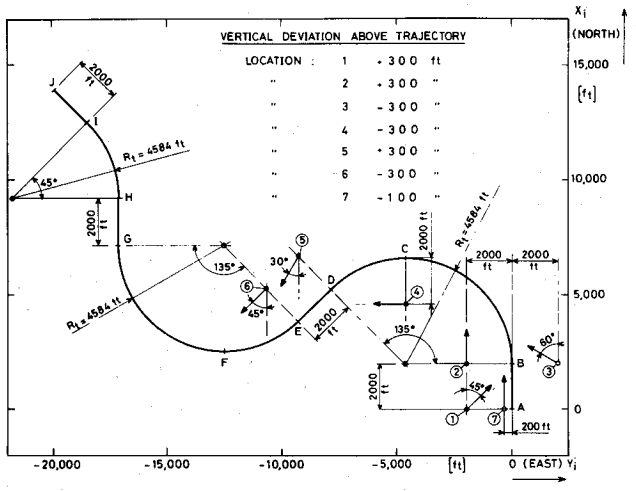

Fig. 6 Planview of desired trajectory.

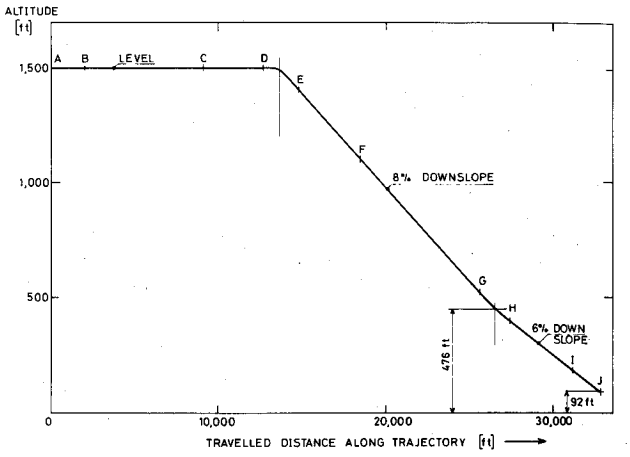

Fig. 7 Descent profile of desired trajectory.

1) Trajectory following in the presence of random lateral and vertical atmospheric disturbances. The subjects were instructed to minimize the lateral and vertical deviations from the trajectory with minimum control effort. Each run started from initial location 7 with an initial lateral deviation of 200 ft to the left of the trajectory, a vertical deviation of 100 ft below the trajectory and zero intercept angle. Thus control action was required from the subject, immediately after starting the simulation run, to bring the vehicle back on the trajectory. The lateral gust disturbance components v_g (lateral velocity gust), and p_g (roll-rate gust) and the longitudinal gust disturbance components u_g (forward velocity gust), and w_g (vertical velocity gust) were generated by passing band-limited white noise with a band limit of 1.5 Hz through first-order shaping filters. The rms values were as follows: v_g-13.5 ft/s, p_g-0.086 rad/s, u_g-9.0 ft/s, and w_g-12.2 ft/s, and the break frequency of all shaping filters was 0.2 rad/s. In order to simulate slow-varying cross and head winds together with gust disturbances, the break frequency of the shaping filters was chosen to be one decade lower than commonly used turbulence models.

Each run lasted 128 s, during which the means and autocovariances of deviations, state variables, and control commands were computed.

2) Trajectory entry. This experiment attempted to simulate a sudden confrontation with the situation of being located outside the trajectory by entering the trajectory from a randomly chosen unknown location. The subjects were instructed to bring the vehicle back on the desired trajectory, as quickly as possible, as smoothly as possible, and with minimum control effort. Gust disturbances were not present in this experiment. In order to prevent the subject from knowing his initial position before the start of a simulation run, the display was initially blanked and was made visible only immediately after starting the simulation run.

Each run started randomly from one of the six initial locations shown in Fig. 6. For all locations the initial lateral deviation was 2000 ft to the left or right of the trajectory and the initial vertical deviation was 300 ft above or below the trajectory. The initial intercept angle was set between 0 and 60 deg.

Each entry run lasted 38.4 s during which the following performance scores were computed:

1) The lateral settling time T_{sl} defined as the time from the start of the run to the moment the lateral deviation settles within a ± 100 ft settling tolerance about the desired trajectory and the vertical settling time T_{sv}, for which the settling tolerance is ± 75 ft.

2) The means and autocovariances of deviations, state variables, and control commands.

3) The lateral deviation score, defined as the averaged absolute value of the lateral deviation, computed between $t=T_1$ and T_2, where $T_1 = 10\,s$ *and* $T_2 = 38.4$ s, according to

$$sc(y_d) = \frac{1}{(T_2 - T_1)} \int_{t=T_1}^{T_2} |y_d| dt \qquad (1)$$

The vertical deviation score was computed in the same way as the lateral one. The lateral and vertical deviation scores were chosen to be averaged absolute values rather than averaged squared values in order to prevent these scores from being dominated by the large initial deviation. For the same reason, the averaging process started at $t=T_1$ s. T_1 is chosen to be about 25% less than the best possible settling time.

Results of Simulations with the Low-Cost Simulation System

Four nonpilot subjects participated in the experimental program. Apart from Subject A, all subjects were male. Subjects A, C, and D were aeronautical engineering students with no prior flight or simulator training and subject B was an aeronautical engineer with extensive simulator experience. Each subject participated in 2-3 2 h/week simulation sessions. All subjects reached a stable level of performance after six weeks of training. Subject motivation was largely enhanced by using a reward system, based on a general performance score, composed of the weighted sum of mean-squared deviations and control commands. The reward, given in the form of extra pay, was determined by the performance level which was reached as well as maintained during the session. Although significant differences among the results of the subjects were observed, the general trends were identical. Therefore, within the limited scope of this paper, only the most characteristic results of subject B are presented and summarized in Tables 1 and 2. The complete results of all four subjects are presented in Ref. 16.

Results of Trajectory Following Comparison of the Perspective Vehicle Symbol with the Flat Predictor Cross

In Fig. 8 the lateral scores of subject B are shown as a function of the reference predictor distance D_o, with D_o set to 900, 1500, and 2000 ft. For both the perspective vehicle symbol and the flat predictor cross, the lateral deviation was found to increase strongly with the predictor distance D_0, whereas the roll activity and lateral stick activity were found to decrease strongly. The contribution of the perspective vehicle symbol was found particularly in the markedly lower roll activity over the complete range of D_0, which implies that the pilot reduces his gain and, thereby, the perspective vehicle symbol contributes to the roll damping. On the other hand,

Table 1 Results of trajectory following: subject B

	"Upright" tunnel; 300 ft wide, roll version								"Banked" tunnel		
	Flat predictor cross, D_0			Perspective vehicle symbol, D_0			Manual throttle perspective symbol $D_0 = 1500$ ft		Perspective symbol $D_0 = 1500$ ft		
							"tick" marks	Digital readout	300 ft wide Roll version	450 ft wide	300 ft wide Roll stabilized
	900 ft	1500 ft	2000 ft	900 ft	1500 ft	2000 ft					
No. of runs	6	6	6	6	8	6	6	7	6	6	6
Predicted lateral deviation, 10^5 ft^2	0.145[a] ±0.052[b]	1.071 ±0.063	2.143 ±0.235	0.266 ±0.022	0.788 ±0.273	2.253 ±0.338	0.772 ±0.074	0.741 ±0.110	0.670 ±0.061	0.596 ±0.093	–
Predicted vertical deviation, 10^4 ft^2	0.438 ±0.090	2.694 ±0.614	5.469 ±0.824	0.721 ±0.044	2.055 ±0.543	5.980 ±0.925	2.835 ±0.599	3.348 ±0.477	2.073 ±0.254	1.746 ±0.228	–
Lateral deviation, 10^4 ft^2	0.160 ±0.016	0.360 ±0.078	0.299 ±0.063	0.251 ±0.019	0.293 ±0.061	0.374 ±0.095	0.261 ±0.023	0.340 ±0.082	0.236 ±0.028	0.374 ±0.062	0.272 ±0.014
Vertical deviation, 10^3 ft^2	0.501 ±0.115	1.056 ±0.593	1.257 ±0.378	0.581 ±0.092	1.065 ±0.196	1.774 ±0.534	1.333 ±0.565	1.519 ±0.413	0.974 ±0.145	1.010 ±0.192	0.896 ±0.157
Bank angle, rad^2	0.151 ±0.005	0.138 ±0.005	0.138 ±0.001	0.143 ±0.004	0.131 ±0.005	0.134 ±0.003	0.140 ±0.004	0.149 ±0.004	0.134 ±0.002	0.129 ±0.003	0.134 ±0.003
Bank angle rate, 10^{-2} (rad/s)^2	0.987 ±0.095	0.667 ±0.068	0.595 ±0.069	0.637 ±0.102	0.375 ±0.102	0.311 ±0.034	0.397 ±0.073	0.567 ±0.085	0.374 ±0.027	0.284 ±0.023	0.457 ±0.064
Velocity error, 10^2 (ft/s)^2	–	–	–	–	–	–	0.492 ±0.212	2.718 ±1.455	–	–	–
Throttle displ. 10 (ft/s^2)^2	–	–	–	–	–	–	0.996 ±0.240	2.733 ±0.604	–	–	–
Lateral stick, 10^{-1} rad^2	1.252 ±0.165	0.930 ±0.147	1.004 ±0.327	0.998 ±0.218	0.581 ±0.325	0.725 ±0.219	0.841 ±0.201	0.993 ±0.170	0.687 ±0.142	0.780 ±0.160	0.991 ±0.144
Forward stick, 10^{-1} rad^2	0.446 ±0.199	0.226 ±0.052	0.488 ±0.158	0.228 ±0.030	0.234 ±0.033	0.407 ±0.156	0.359 ±0.093	0.495 ±0.144	0.387 ±0.133	0.498 ±0.088	0.539 ±0.129

[a] Average of n scores. [b] Standard deviation of n scores. Each score is the autocovariance of variable x computed as: $\text{cov}(x) = \frac{1}{T}\int_0^T x^2 dt$.

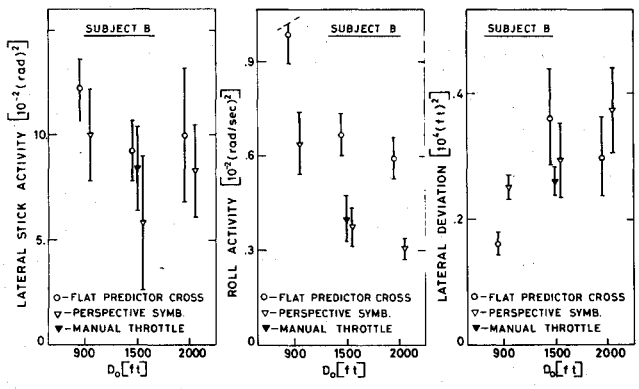

Fig. 8 Lateral results of trajectory following as a function of reference predictor distance D_0, subject B.

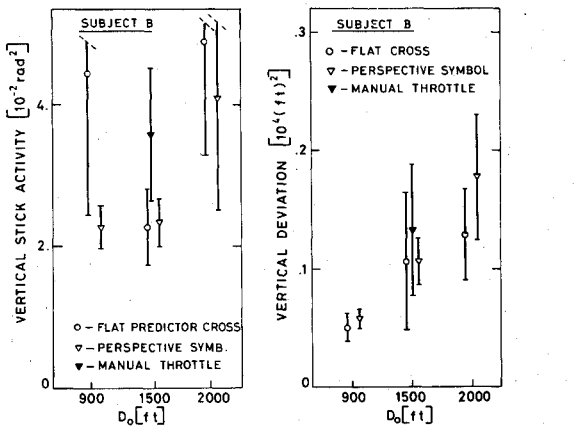

Fig. 9 Vertical results of trajectory following as a function of reference predictor distance D_0, subject B.

the perspective vehicle symbol yielded a somewhat larger lateral deviation with predictor distances of 900 and 2000 ft, but a smaller deviation with predictor distance of 1500 ft. In the vertical axis of control these effects were less pronounced. The vertical results of subject B are shown in Fig. 9 and indicate that also the vertical deviation strongly increased with D_0. The perspective vehicle symbol yielded a somewhat larger vertical deviation than the predictor cross, which might be attributed to the fact that the vehicle symbol with its complex shape is harder to match to the tunnel square.

Results of Manual Velocity Control

The results of the auto-throttle control and manual velocity control by means of velocity tick-marks are compared in Figs. 8 and 9. Neither in the lateral nor in the vertical axis of control did the results for the manual throttle differ significantly from the results for the auto-throttle, which suggests that velocity control could be carried out without affecting the tunnel following performance.

For comparison, manual velocity control was carried out also by means of the digital velocity readout presented in the lower center of the display, as shown in Fig. 1. In this experiment the predictor distance was kept constant at $D = D_0$ regardless of the variations in velocity. In contrast with velocity control by means of the tick-marks, velocity control by means of the digital readout yielded a markedly deteriorated tunnel following performance, as seen by the significantly larger roll activity and lateral and vertical deviations, and also by the significantly larger velocity error

Table 2 Results of trajectory entry: subject B

"Upright" tunnel, 300 ft wide, roll version		
Predictor	Flat cross	Perspective symbol
No. of series of 6 runs	6	7
Lateral settling time, 10^2 s	0.207[a] ±0.009[b]	0.206 ±0.006
Vertical settling time, 10^2 s	0.129 ±0.004	0.142 ±0.013
Lateral entry score, 10^3 ft^2	0.213 ±0.019	0.216 ±0.011
Vertical entry score, 10^2 ft^2	0.296 ±0.025	0.368 ±0.022
Bank angle[c] rad^2	0.197 ±0.004	0.195 ±0.002
Bank angle rate,[c] 10^{-2}(rad/s)^2	0.331 ±0.018	0.238 ±0.020
Lateral stick deflection,[c] 10^{-1} rad^2	0.226 ±0.013	0.164 ±0.013
Forward stick deflection,[c] 10^{-2} rad^2	0.644 ±0.053	0.638 ±0.049

[a] Average of n scores.
[b] Standard deviation of n scores.
[c] Scores of these variables are the autocovariances computed as: $\text{cov}(x) = 1/T\int_0^T x^2\,dt$.

autocovariance and throttle activity (see Table 1). These findings are confirmed by the time histories shown in Fig. 10, which show large overshoots in velocity error and throttle displacement and clearly demonstrate the lack of damping for velocity control with digital readout.

Results of the Banked Tunnel

The banked tunnel was investigated, both in the roll-version and the roll-stabilized version. The performance of the roll-version of the banked tunnel was very similar to results of the straight tunnel, see Table 1. The subjects commented that, in the roll-version, the bank-angle command information provided by the tunnel elements banked in curves did not contribute much to the following performance and was ignored in most cases. Furthermore, the bank-angle command was correct only after entering a steady, coordinated turn. In transients to curved sections the bank-angle command was found to be confusing, since setting the bank-angle at the commanded value did not necessarily bring the lateral deviation error to zero.

The roll-stabilized version of the banked tunnel yielded generally larger lateral deviations and roll-activity than the roll-version, see Table 1. This was attributed to the fact that the actual ank angle, which in the roll-version is displayed by the inclination of the horizon, is no longer available in the roll-stabilized version. The predicted bank-angle displayed by the vehicle symbol clearly was not sufficient for obtaining a satisfactory response.

Effect of Tunnel Width

The results for a tunnel enlarged to a width of 450 ft are shown in Table 1. For subject B the roll-activity was significantly lower and the lateral deviation was significantly larger for the 450 ft tunnel than for the 300 ft tunnel. This indicates a decrease in pilot gain on the lateral deviation. The subjects commented that the 450 ft tunnel generally was easier to control than the 300 ft tunnel.

Results of Trajectory Entry

The entry experiment was conducted in a series of six runs. For each run the initial location was chosen at random and without replacement from the set of six initial locations given in Fig. 6. Marked differences between the scores were observed for the various initial locations. In order to rate the general entry performance, a series score was computed by averaging the results of the six series of runs were performed. The entry results of subject B are summarized in Table 2 and represent the average and standard deviation of sets of at least six series scores.

The autocovariances of roll-rate and lateral stick deflection tended to be lower for the perspective vehicle symbol than for the flat predictor cross, whereas no difference in lateral score and lateral settling time was found between the two configurations. This indicates that the perspective vehicle symbol yields a reduced pilot gain and roll damping without affecting the quality of the entry.

The vertical results in Table 2 clearly show a larger vertical score for the perspective vehicle symbol, which might be explained by the fact that the perspective symbol is harder to match to the tunnel square. However, the vertical stick activity is the same for both configurations, indicating that the perspective vehicle symbol does not contribute to a better vertical entry performance.

Results of Simulations with the B-737 Full-Scale Cockpit

The purpose of these simulations was to obtain a preliminary subjective evaluation of the display presented in an authentic flight environment flown by experienced research pilots. The program was limited to 5-6 sessions of 4 h each, during which two pilots performed one training session and several evaluation sessions each. No quantitative data collection took place and pilot acceptance and comments are summarized hereafter.

The pilot subjects found the perspective vehicle symbol more difficult to become familiar with than the flat predictor cross. After familiarization with the display, the predicted pitch and yaw attitude angles were found useful. However, the roll motions of the predictor symbol were found to be disturbingly large and rapid, since the predicted bank-angle was composed of both actual bank-angle and bank-angle rate. It was found preferable to reduce the bank-angle rate portion of the prediction considerably, or even to bring this portion to zero. The predicted bank-angle was obtained by a first-order Taylor series approximation according to Eq. (A7). However, it is shown in Ref. 16 that in a higher order approximation the bank-angle rate portion of the prediction is about ten times smaller than the one in a first-order approximation. The pilot's preference for a smaller bank-angle rate portion of the prediction thus indicates that the first-order prediction of Eq. (A7) is inadequate and a higher-order approximation is required.

The following parameters were varied: 1) reference predictor distance D_o, 2) tunnel width, 3) predictor size, and 4) trajectory curvature. At a nominal airspeed of 130 knots, the most acceptable predictor distance was between 900 and 1250 ft, corresponding to a prediction time between 3.7 and 5.1 s. A tunnel width of 450 ft and a perspectve vehicle symbol with a wing span of 80% of the tunnel width was found adequate. Two trajectories were tested: a strongly curved path yielding steady-state bank angles of about 27 deg and a moderately curved path yielding steady-state bank angles of about 16 deg. Although the strongly curved path yielded bank angles which normally would not appear in actual flight, the path was still easy to fly and deviations still remained within a ± 50 ft tolerance.

Manual velocity control by means of velocity tick-marks proved successful. Accurate velocity control was obtained without overshoots and with minimal throttle activity. All pilots stated that the manual velocity control neither made the overall task more difficult, nor affected the tunnel following performance.

The banked tunnel was investigated both for the roll-version and the roll-stabilized version. The roll-stabilized

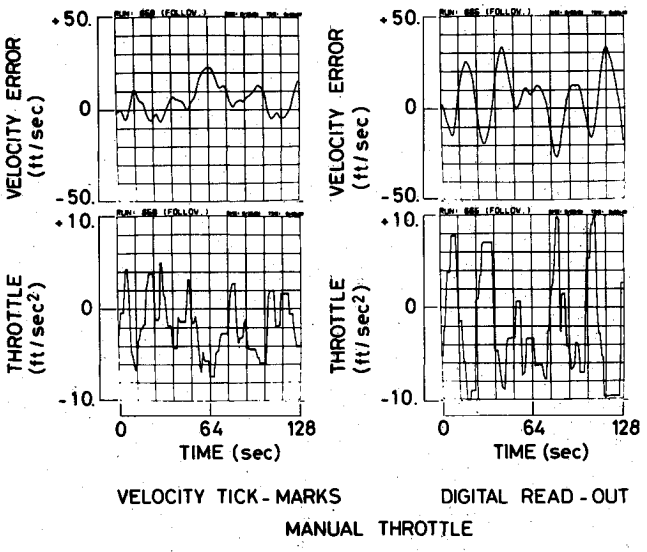

Fig. 10 Time histories of velocity error and throttle position for trajectory following; velocity tick-marks compared with digital readout, subject B.

version was found preferable due to the fact that the bank-angle command was perceived directly as the inclination of the tunnel elements with respect to a stabilized horizon, and thus with respect to the monitor frame rather than to a rolling horizon. Favorable opinion was given to the fact that in a steady coordinated turn the wings of the perspective vehicle symbol were parallel to the tunnel square.

Two main problems were encountered.

1) Variations in the vertical path-angle were excessively large. These variations might be attributed both to the fact that the path-angle is not displayed explicitly and to the fact that the vertical visual angle is too large for accurate vertical control. However, a reduced vertical visual angle also will require a proportional reduction in lateral visual angle, if the image is shown on a monitor with the same dimensions. A reduction of the lateral visual angle will place the tunnel partially outside the field-of-view. Future research efforts should deal with the augmentation of the display with superimposed symbology, explicitly displaying the vertical path-angle in enlarged scaling. The symbology should be located such that it neither interferes with the lateral axis of control, nor clutters existing symbology and yet is located as centrally as possible on the display.

2) In the lateral axis of control, transients to and from curved sections of the path were too sudden. Pilots commented that although the lateral axis of control was very satisfactory in straight sections as well as in steady curves, the transients from straight to curved sections were too sudden. This resulted from the fact that the curvature along the trajectory was varied in steps, without transients from one section to the other. Future developments should deal with the definition of higher-order continuous functions for the trajectory curvature and commanded bank-angle. These functions should be matched to the average vehicle response and must enable the pilot to follow the trajectory through straight, transient, and curved sections by setting the bank angle at the commanded value.

Conclusions

1) The perspective vehicle symbol requires a longer time to become familiar with than the flat predictor cross.

2) The perspective vehicle symbol yields a smaller roll activity and thus contributes to the lateral system damping, but yields generally larger vertical deviations.

3) The perspective vehicle symbol with velocity tick-marks enables accurate velocity control, without overshoots, with moderate throttle activity and without affecting the tunnel following performance.

4) A tunnel width of 450 ft and perspective vehicle symbol with a wing span of 80% of the tunnel width yield the best pilot acceptance. This dimension is acceptable only for the curved enroute section of the approach, which is well above decision height.

5) The advantage of the perspective vehicle symbol over the flat predictor cross is marginal, particularly since the flat predictor cross already yields a satisfactory response. In cases in which the computation power of the graphics system is limited, the flat predictor cross is recommended.

6) The present display configuration lacks the ability to control the vertical path-angle adequately. Explicit display of the vertical path-angle in enlarged scaling is recommended.

7) The banked tunnel in the present configuration is effective only in a steady coordinated turn. Incorrect bank-angle commands in transients to curved sections are confusing. In order to be effective in transients as well, it is recommended that the functions for trajectory curvature and commanded bank angle are continuous and are matched to the average vehicle response.

Appendix

Predictor Motions Laws

The perspective vehicle symbol is located with its center of gravity on the predicted vehicle path, a distance D ahead of the vehicle and with the longitudinal body axis x_p tangential to the path, see Fig. A1. The predicted vehicle path is assumed to be tangential to the velocity vector of the vehicle $\vec{V}$. The projections of this path on the $x_i y_i$ locally level plane and on the $x_i z_i$ locally vertical plane are hereafter referred to as the lateral and vertical vehicle path, respectively, and are computed from the lateral and vertical path accelerations, a_l and a_v, respectively. Assuming these accelerations remain constant over the prediction span, circular lateral and vertical vehicle paths are obtained. The instantaneous lateral and vertical path-angle rates $\dot{\chi}$ and $\dot{\xi}$ are computed from

$$\dot{\chi}(t) = a_l(t)/V \tag{A1}$$

and

$$\dot{\xi}(t) = a_v(t)/V \tag{A2}$$

respectively. The situation for the horizontal path is shown in Fig. A1. The actual path-angle and lateral deviation are denoted by χ and y_d, respectively, and the predicted path-angle and predicted lateral deviation by χ_p and y_{d_p}, respectively. For the relatively small heading angle ψ, sideslip angle β, and path-angle χ, the predicted path-angle and lateral deviation Ts in the future, are given by

$$\chi_p(t) = \chi(t) + \nu(t) \tag{A3}$$

$$y_{d_p}(t) = y_d(t) + D\chi(t) + D\frac{\nu(t)}{1+\sqrt{1-\nu(t)^2}} \tag{A4}$$

where

$$\nu(t) = T\dot{\chi}(t) \tag{A5}$$

In a steady turn, the radius of the vehicle path will become equal to the radius of the trajectory which enables a zero steady-state error in the lateral deviation.

The equations for the vertical vehicle path are identical to Eqs. (A3) and (A4). Since constantly curved sections usually do not exist in the vertical profile of the trajectory, the third term in Eq. (A4) can be linearized and the predicted deviation becomes

$$z_{d_p}(t) = z_d(t) + D\xi(t) + \frac{1}{2}\frac{D^2}{V}\dot{\xi}(t) \tag{A6}$$

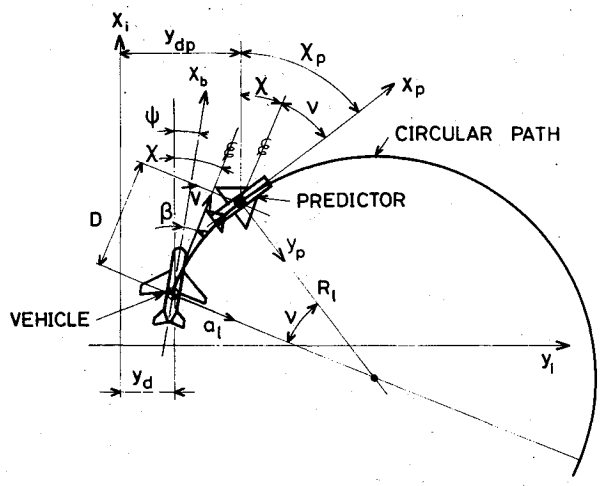

Fig. A1 Horizontal situation of circular predicted vehicle path.

It is shown in Ref. 16 that by using Eq. (A4) or (A6) as the control error, the open-loop transfer function is furnished with a pair of complex zeros with a fixed damping ratio of $\zeta = 0.707$ and a natural frequency $\omega_n = 1/T$. Thus the amount of phase lead increases with T. Since the transfer function for the vertical axis of control is effectively of a higher bandwidth than the lateral one, less phase lead is required to stabilize the system. Therefore, the prediction time for the vertical path was chosen 0.2 times the prediction time for the lateral path.

Note that the angular orientation of the predictor symbol indicates future path angles rather than future attitude angles. However, since the angle of attack and sideslip angle remain small (also in the future), the difference is negligible.

The predicted bank angle ϕ_p is obtained by a first-order Taylor series approximation according to

$$\phi_p(t) = \phi(t) + T\dot{\phi}(t) \tag{A7}$$

Predictor Laws for Forward Velocity Control

For a given prediction time T, the predictor distance D can be computed from the present states of the longitudinal dynamics and from the present control commands. Since the engine and velocity control dynamics are of a much lower natural frequency than the short-period longitudinal dynamics, the computation of D can be simplified. The engine dynamics are represented by a first-order lag with time constant $1/c$ s, given by

$$\dot{a}_x = -ca_x + k\delta_{th} \tag{A8}$$

where a_x is the forward acceleration due to engine thrust, and δ_{th} is the throttle position. The component of $\bar{V}$ in forward body-axis direction is denoted by U which is the integral of a_x, while the traveled distance S is the integral of U. Assuming δ_{th} remains constant over the prediction span, a linear prediction of S, τ s in the future, from the present time t onward is given by

$$S(t+\tau) = \frac{1}{c^2}(e^{-c\tau} + c\tau - 1)a_x(t) + \tau U(t) +$$

$$+ S(t) - \frac{k}{c^3}\left(e^{-c\tau} - \frac{c^2\tau^2}{2} + c\tau - 1\right)\delta_{th}(t) \tag{A9}$$

For $\tau = T$ the predictor distance D is given by

$$D = S(t+T) - S(t) \tag{A10}$$

Expanding the exponential term in Eq. (A9) to the third derivative and substituting Eq. (A9) in Eq. (A10) yields:

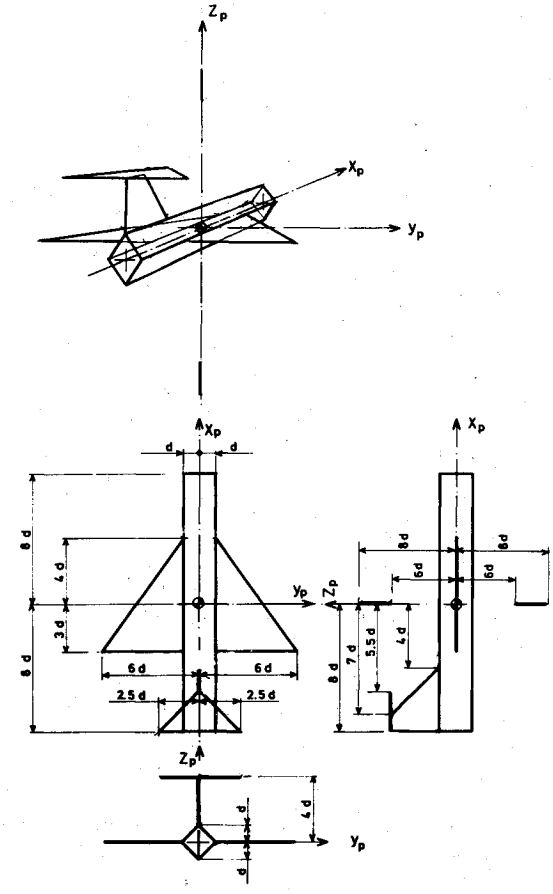

Fig. A2 Graphical description of perspective vehicle symbol.

$$D = TU(t) + \left(\frac{T^2}{2} - c\frac{T^3}{6}\right)a_x(t) + \frac{T^3}{6}k\delta_{th}(t) \tag{A11}$$

The vehicle symbol with velocity tick-marks will be positioned at distance D ahead, whereas the solid reference square at distance $D_0 = TU_0$ ahead, where U_0 is the desired velocity. The velocity U is brought to the desired value U_0 by bringing the distance between D and D_0 to zero. It is shown in Ref. 16 that Eq. (A11) provides the system with complex zeros with a fixed damping ratio of $\zeta = 0.61$ and natural frequency $\omega_m = 2.45/T$. Since the velocity control system is effectively of a much lower bandwidth than the lateral or vertical axis of control, more phase lead is required and the prediction time for velocity control is chosen twice the prediction time for the lateral path.

The effect of variations in U is strongly observed in apparent changes in size of the predictor symbol. Thus, an increase in U yields an increase in D, which is manifested in an apparent shrinking in size of the vehicle symbol. On the other hand, a decrease in U yields an apparent increase in size of the vehicle symbol. Equation (A11) also shows that an increase in engine thrust, due to a forward throttle displacement, results in a simultaneous forward motion of the vehicle symbol so that throttle displacement and vehicle symbol motion are in the same direction.

Graphical Description of the Perspective Vehicle Symbol

A graphical description of the perspective vehicle symbol is given in Fig. A2. The fuselage cross-section is square and box-shaped while the wings and tail are triangular, in order to visualize the pitch motion clearly.

In order to obtain an unambiguous vehicle symbol, the hidden lines should be removed from the image. However, commonly used algorithms for removing hidden lines require considerable computational efforts which might influence the

update rate unfavorably. An alternative fast method has been developed to remove hidden lines without requiring additional CPU time. A description of this method is given in Ref. 16. The hidden-line removal is restricted to the fuselage structure. Thus the fuselage appears "solid," but the wings and tail still appear transparent. In spite of these restrictions a clear and unambiguous image is obtained with minimal computational effort.

Acknowledgments

This research was sponsored by NASA under Contract NASW-3302, under the technical direction of S.A. Morello of Langley Research Center, Hampton, Va. This research has been carried out as a joint program between Langley Research Center and The Technion—Israel Institute of Technology, Haifa, Israel, in the framework of the Terminal Configured Vehicle (TCV) program at NASA Langley Research Center. The quantitative evaluation with low-cost visual simulation system and nonpilot subjects took place at the Technion, whereas the qualitative evaluation with experienced research pilots was carried out with the full-scale Boeing 737 cockpit at Langley Research Center. The author wishes to thank S. A. Morello for making the use of the simulation system at Langley Research Center possible, as well as for his valuable comments, and L. E. Person and J. B. Robertson for their participation as evaluation pilots.

References

[1]Sidorsky, R. C. and Allen, F. L., "Ship Control-9 an Evaluation of a Horizon-at-Infinity in a Contact Analog Display," General Dynamics Corp., Electric Boat Div., Groton, Conn., Aug. 1958.

[2]LaRussa, J. A., "A Multi-Purpose Wide Field, Three-Dimensional Head-Up Display for Aircraft," Farrand Optical Company, Inc., Valhalla, New York, 1960.

[3]Van Houtte, N. A. J., "A Perspective Glideslope Indicating System," *6th Annual Conference on Manual Control*, April 1970, pp. 117-131.

[4]Eisele, J. E., Willeges, R. C., and Roscoe, S. N., "The Isolation of Minimum Sets of Visual Image Cues Sufficient for Spatial Orientation During Aircraft Landing Approaches," Aviation Research Laboratory, University of Illinois at Urbana-Champaign, Savoy, Ill., Nov. 1976.

[5]Murphy, M. R. and Greif, R. K., "Simulator Evaluation of a Perspective Clipped-Pole Display and Thrust-Vector Controller for VTOL Zero-Zero Landings," *11th Annual Conference on Manual Control*, May 1975, pp. 268-283.

[6]Wilckens, V., "Improvements in Pilot/Aircraft Integration by Advanced Contact Analog Displays," 9th Annual Conference on Manual Control, May 1973.

[7]Schattenmann, W. and Wilckens, V., "Comparative Simulator Studies with the Contact Analog Channel Display and with Conventional Instruments," European Space Research Organization, ESRO TT-15, Feb. 1974.

[8]Knox, C. E. and Leavitt, J., "Description of Path-in-the-Sky Contact Analog Piloting Display," NASA TM-74057, Oct. 1977.

[9]Kraiss, K. F. and Schubert, E., "Comparative Experimental Evaluation of Two-Dimensional and Pseudo-Perspective Displays for Guidance and Control," Research Institute for Human Engineering, Buschstrausee, Germany, Nov. 1976.

[10]Adams, J. J. and Lallman, F. J., "Description and Preliminary Studies of a Computer Drawn Instrument Landing Approach Display," NASA TM-78771, Nov. 1978.

[11]Kelley, C. R., "Developing and Testing the Effectiveness of the Predictor Instrument," Dunlap and Associates, Inc., Tech. Rept. 252-60-1, March 7, 1960.

[12]Smith, R. L. and Kennedy, R. S., "Predictor Displays: History, Research, and Applications," Pacific Missile Test Center, Point Mugu, Calif., Tech. Pub. 76-05, June 1975.

[13]Smith, R. L. and Kennedy, R.S., "Predictor Displays: A Human Engineering Technology In Search of a Manual Control Problem," Pacific Missile Test Center, Point Mugu, Calif., June 1976.

[14]Grunwald, A. J., Robertson, J. B., and Hatfield, J. J., "Experimental Evaluation of a Perspective Tunnel Display for Three-Dimensional Helicopter Approaches," *Journal of Guidance and Control*, Vol. 4, Nov.-Dec. 1981, pp. 623-631.

[15]McRuer, D., Ashkenas, I., and Graham, D., *Aircraft Dynamics and Automatic Control,* Princeton University Press, N. J., 1973, pp. 711-717.

[16]Grunwald, A.J., "Predictor Symbology in Computer-Generated Pictorial Displays," Technion Aeronautical Engineering Dept., Technion, Haifa, Israel, TAE Report 470, Nov. 1981.